Macromolecules
ARTICLE

*Macromolecules* **2009**, *42*, 9161–9169 **9161**
DOI: 10.1021/ma901849j

# Preparation of Temperature-Sensitive Core−Shell Poly(glycidol)/Poly(*N*-isopropylacrylamide) Nanohydrogels under Surfactant-Free Conditions

**Sebastian Mendrek,[†,‡] Aleksandra Mendrek,[†,‡] Hans-Jürgen Adler,[†] Andrzej Dworak,[‡] and Dirk Kuckling*[,†,§]**

[†]*Fachrichtung Chemie und Lebensmittelchemie, Technische Universität Dresden, D-01062 Dresden, Germany,* [‡]*Center of Polymer and Carbon Materials, M. Sklodowskiej-Curie 34, 41-819 Zabrze, Poland, and* [§]*Department Chemie, Universität Paderborn, Warburgerstrasse 100, D-33098 Paderborn, Germany*

*Received August 19, 2009; Revised Manuscript Received September 23, 2009*

ABSTRACT: A new method for synthesis of smart nanohydrogels under additives-free conditions and at high solid content is presented. The new core−shell nanohydrogels with cross-linked poly(*N*-isopropylacrylamide) (PNIPAAm) core and hydrophilic poly(glycidol) (PGl) shell were obtained by photo-cross-linking of PGl-*b*-PNIPAAm copolymers above their phase transition temperature ($T_c$). As UV-active group, the chromophore 2-(dimethylmaleimido)-*N*-ethylacrylamide (DMIAAm) was synthesized and successfully incorporated in the PNIPAAm segment, while poly(glycidol) chains were responsible for stability of aggregates above $T_c$. Photo-cross-linkable block copolymers with different PGl length (DP = 55 and 100), DMIAAm chromophore content, and PGl/PNIPAAm block ratio were synthesized for this investigation. It was found that the efficacy of cross-linking strongly depended on the length of PGl block in the copolymer. In the case of copolymers with shorter PGl chains formation of fully cross-linked nanohydrogels was observed already at 45 °C, while for copolymers with longer PGl chains monomodal nanohydrogels were formed at 55 °C. In contrast at given temperature, the rate of cross-linking was independent of chromophore content in copolymer and copolymer composition.

## Introduction

In recent years, considerable interest has been focused on the development of so-called *smart* hydrogels. Such hydrogels exhibit sensitivity in terms of their swelling behavior as response to changes in environmental conditions like temperature, pH, ionic strength, etc.[1,2] Among this big group of polymeric materials, temperature-sensitive nanohydrogels based on poly(*N*-isopropylacrylamide) (PNIPAAm) have gathered great interest.[3−8] PNIPAAm hydrogels are known for their reversible swelling−deswelling behavior in response to temperature changes across the volume phase transition temperature ($T_c$). Hence, PNIPAAm-based nanohydrogels are being considered for use in various devices, including switches, sensors, chemomechanical actuators, drug delivery devices, recyclable absorbents, specialized separation systems, bioreactors, catalysis, etc.[5−8] However, there is a demand for the preparation of temperature-sensitive nanohydrogels with specific properties, e.g., stability, well-defined, uniform microstructure, and desired response time.

One of the most important properties of smart nanohydrogels for potential applications is their swelling−deswelling behavior. Swelling and deswelling are diffusion-controlled processes.[9] The so-called response time of the swelling/deswelling process is dependent on nanohydrogel size and the cooperative diffusion coefficient. Since the cooperative diffusion coefficient is a material constant, the decrease of hydrogel size has been considered to be the best way to obtain products with sufficient response times. In other words, the slow dynamics of the swelling/deswelling process in macroscopic hydrogels can be overcome and accelerated by the preparation of nanohydrogel particles with dimensions in the submicrometer range.

Another important feature of nanohydrogels in terms of future application is the presence of functional groups within their structure. In principle, the functionalization of nanohydrogels can combine several objectives. By incorporation of functional groups volume phase transition behavior of nanohydrogel can be controlled, where both the absolute value of $T_c$ and the width of the swelling transition can be influenced. Functionalization can also provide reactive sites for postmodification of the nanohydrogel. The distribution and accessibility of functional groups are critical in determining the types of applications; for example, nanohydrogels designed for attachment of other substances like enzymes or proteins would contain functional groups at or near the nanohydrogel surface, accessible for chemical reactions. On the contrary, nanohydrogels targeted for drug delivery applications should contain internal functional groups whose access is diffusion-controlled.

The stability of nanohydrogels at elevated temperature higher than $T_c$ is also of great interest. It is known that nanohydrogel stability can be improved by introduction of surfactants into the system or by introduction of ionic or neutral hydrophilic groups into nanohydrogels structure.[4] The increase of the stability can also be obtained by the preparation of particles with well-defined core−shell morphology, where the cross-linked core is stabilized by a hydrophilic corona. Then, the hydrophilic free chains surrounding the cross-linked core are acting as steric stabilizers, and the particles are remained dispersed over the whole temperature range.[4]

The most common method of PNIPAAm nanohydrogel synthesis is the free radical polymerization of NIPAAm, in water

*Corresponding author. E-mail: dirk.kuckling@uni-paderborn.de.

© 2009 American Chemical Society

Published on Web 10/12/2009

in the presence of different additives, e.g., surfactants, stabilizers, and cross-linker, under emulsion polymerization conditions. Using this method, homo-PNIPAAm[10−12] nanohydrogels and core−shell PNIPAAm nanohydrogels were prepared by a number of research groups.[13−15] However, the synthesis of nanohydrogels by free radical emulsion polymerization inheres a lot of difficulties, making synthesis of well-defined functionalized products complicated. First of all, it could be shown that the commonly used cross-linker *N*,*N*′-methylenebis(acrylamide) has a higher polymerization rate than NIPAAm. Thus, nanohydrogel particles did not grow uniformly. The distribution of cross-linker radially decreased in the particles strongly influencing their properties.[16,17] In addition, usually during nanohydrogel formation a significant amount of sol fraction (i.e., unreacted monomer, linear or slightly branched polymers) remains and must be removed by dialysis, which requires sophisticated dialysis equipment and is time-consuming. The removal of surfactants, which are crucial for the stabilization of polymer system above the critical temperature, is also a challenging task. It has been shown that surfactant molecules bond to nanohydrogel structure, influencing their swelling−deswelling behavior and leading to significant increase in $T_c$ of PNIPAAm nanohydrogels.[18] In some cases due to the binding of surfactants the elimination of temperature sensitivity of nanohydrogels was observed.[19]

One alternative preparation method of PNIPAAm nanohydrogels has been recently developed.[20,21] On the basis of the coil−globule transition phenomenon, stimuli-sensitive photo-cross-linkable PNIPAAm homopolymers or graft copolymers containing incorporated 2-(dimethyl maleimido)-*N*-ethylacrylamide chromophore (DMIAAm) have been heated above phase separation temperature and cross-linked by exposure to UV light. By random distribution of chromophores in the polymer backbone, spatial inhomogeneities caused by differences in cross-linking density were eliminated.[22] However, the presence of surfactant was necessary in order to stabilize formed aggregates at elevated temperatures.

In some cases the formation of nanohydrogels occurred under surfactant-free conditions without the introduction of chemical cross-linker into the system using self-cross-linking as the result of chain transfer reaction[23] or by $\gamma$-irradiation of linear chains.[24] However, the cross-linking had to be carried out at highly diluted solutions to suppress extensive intermicellar cross-linking, which strongly influences yield of nanohydrogels synthesis.

In order to avoid the presence of surfactants but retain colloidal stability of PNIPAAm nanohydrogels above $T_c$, PNIPAAm nanohydrogels containing hydrophilic PEO segments were prepared by simultaneous copolymerization of NIPAAm with PEO macromonomers.[25,26] The introduction of hydrophilic chains improved the swelling−deswelling behavior as well enabling the control of $T_c$ and the width of the swelling transition. However, despite high solubility, biocompatibility, and stability of PEO, the lack of functional groups set the limits for PNIPAAm−PEO nanohydrogels as a material for more complex structures.

An alternative way to form core−shell particles utilizes the self-assembly process of block copolymers. In order to stabilize micellar structures, either the shell[27] or the core[28] can be cross-linked. For the preparation of nanohydrogels the formation of core cross-linked micelles would be applicatory because the structures can be prepared from tailor-made and well-defined polymers. Especially the combination with photo-cross-linking would lead to a controllable cross-linking process.[29,30]

The goal of this work was the surfactant-free synthesis of monodispersed, uniform, submicrometer size, stable, core−shell PNIPAAm nanohydrogels bearing easily available functional groups suitable to postmodification. Poly(glycidol) (PGl), a highly hydrophilic polymer which can be referred as a functional analogue of PEO, where one of the hydrogen atoms in the chain repeating unit was replaced with a $CH_2OH$ group, was introduced into the shell of PNIPAAm nanohydrogels. The general idea applied in our studies involved the temperature-induced organization of well-defined PGl-*b*-PNIPAAm block copolymers bearing randomly localized chemical functionalities (chromophores DMIAAm) into aggregate assemblies, followed by UV-induced cross-linking of collapsed PNIPAAm chains. In this approach stable aggregates were formed, while the stabilization above phase separation temperature was derived from the highly hydrophilic PGl shell. The applied strategy is presented schematically in Figure 1.

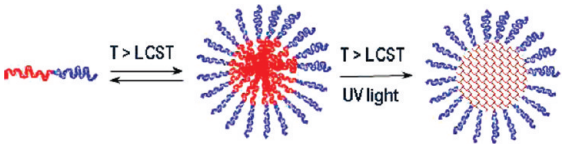


**Figure 1.** Synthetic approach used upon preparation of PGl/PNIPAAm core−shell nanohydrogels.

## Materials and Methods

**Materials.** Dimethylformamide (DMF) (Fluka) and 1,4-dioxane were freshly distilled before use. Other solvents were used as received. Acryloyl chloride (Merck, 96%) was distilled prior to use. Triethylamine (TEA) (Fluka, 98%) was distilled over $CaH_2$ prior to use. *N*-Isopropylacrylamide (NIPAAm) was recrystallized three times from distilled hexane and stored at 4 °C. Di-*tert*-butyldicarbonate ($(Boc)_2O$) (Acros, 97%,), dimethylmaleic anhydride (Lancaster, 97%), trifluoroacetic acid (Aldrich, 99%), silica gel 60 (Merck, 0.040−0.063 mm), aluminum oxide 90 active neutral (Merck, 0.063−0.200 mm), copper chloride (CuCl) (Aldrich, 99.995%), sodium chloride (J.T. Baker, p.a.), sodium carbonate (J.T. Baker, p.a.), tris(2-aminoethylamine) (TREN) (Aldrich, 96%), formic acid (85% Roth GmbH), and formaldehyde (37%, Roth GmbH) were used as received. $Me_6$TREN was obtained according to a procedure described by Matyjaszewski[31] and stored under a nitrogen atmosphere.

**$Cu^I$-$Me_6$TREN Complex Preparation.** To a small reactor equipped with stir bar and filled with argon 0.11 g (0.48 mmol) of $Me_6$TREN and 0.047 g (0.48 mmol) of CuCl were added. To remove traces of oxygen, the reactor was evacuated and filled with dry argon two times. Then 1.0 mL of degassed water was added, and after stirring for few minutes a dark blue, heterogeneous solution was obtained. Finally, the desired volume of complex solution was transformed into the reactor just before the onset of polymerization.

**Synthesis of Photo-Cross-Linkable PGl-*b*-(PNIPAAm-*r*-DMIAAm) Block Copolymers.** Detailed information on PGl macroinitiator synthesis has been published previously.[32] Poly(glycidol) macroinitiator with DP = 55 and 100 was obtained by living anionic polymerization of protected glycidol followed by esterification of $\omega$-hydroxyl group with $\omega$-(2-chloropropionyl) chloride and removal of protecting group of poly(glycidol). DMIAAm chromophore was synthesized according to a procedure described in the literature.[20]

Photo-cross-linkable PGl-*b*-(PNIPAAm-*r*-DMIAAm) block copolymers were obtained using an analogous procedure as we described previously for PGl-*b*-PNIPAAm copolymers.[32] In order to ensure formation of cross-link points by UV irradiation, the DMIAAm chromophore was incorporated into the PNIPAAm block.

*General Procedure*. 1 g of poly(glycidol) macroinitiator ($PGl_x$, where $x$ refers to DP of poly(glycidol)) was added to a glass reactor and dissolved in degassed DMF (Table 1). Under an argon atmosphere a mixture of NIPAAm and DMIAAm was added into the reactor (Table 1). The required amount of water

**Table 1. Preparation of Photo-Cross-Linkable $PGl_x$-*b*-(PNIPAAm-*r*-$DMIAAm^z)_y$ Copolymers**

| | | *n* [mmol] | | volume [mL] | | | |
|---|---|---|---|---|---|---|---|
| sample | *n* [mmol] of macroinitiator (1 g) | NIPAAm | DMIAAm | water | DMF | catalyst | yield [%] |
| $PGl_{55}$-*b*-(PNIPAAm-*r*-$DMIAAm^{5.2})_{110}$ | 0.24 | 26.5 | 1.3 | 6 | 7 | 1 | 95 |
| $PGl_{55}$-*b*-(PNIPAAm-*r*-$DMIAAm^{4.7})_{160}$ | 0.24 | 40.0 | 2.0 | 9 | 10 | 1 | 95 |
| $PGl_{55}$-*b*-(PNIPAAm-*r*-$DMIAAm^{4.9})_{340}$ | 0.24 | 80.0 | 4.0 | 20 | 21 | 1 | 96 |
| $PGl_{55}$-*b*-(PNIPAAm-*r*-$DMIAAm^{9.0})_{170}$ | 0.24 | 40.0 | 4.0 | 9 | 10 | 1 | 94 |
| $PGl_{55}$-*b*-(PNIPAAm-*r*-$DMIAAm^{9.0})_{280}$ | 0.24 | 80.0 | 8.0 | 20 | 21 | 1 | 89 |
| $PGl_{100}$-*b*-(PNIPAAm-*r*-$DMIAAm^{2.0})_{190}$ | 0.13 | 26.5 | 5.4 | 6.5 | 7 | 0.5 | 95 |
| $PGl_{100}$-*b*-(PNIPAAm-*r*-$DMIAAm^{5.0})_{210}$ | 0.13 | 26.5 | 1.3 | 6.5 | 7 | 0.5 | 95 |
| $PGl_{100}$-*b*-(PNIPAAm-*r*-$DMIAAm^{5.5})_{320}$ | 0.13 | 40.0 | 2.0 | 9.5 | 10 | 0.5 | 97 |
| $PGl_{100}$-*b*-(PNIPAAm-*r*-$DMIAAm^{4.9})_{520}$ | 0.13 | 80.0 | 4.0 | 20.5 | 21 | 0.5 | 85 |

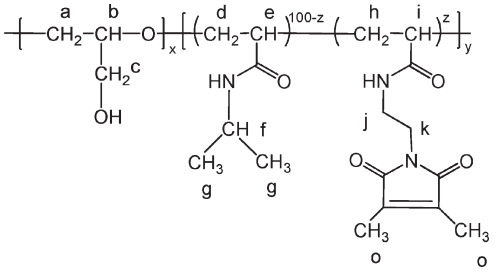


**Figure 2.** Structure of $PGl_x$-*b*-(PNIPAAm-*r*-$DMIAAm^z)_y$ copolymers.

was added, and all was degassed by three freeze−pump−thaw cycles. Next freshly prepared $Cu^I$-$Me_6$TREN complex solution was added. The color turned to light blue. A small exothermic effect ($\Delta T$ = 5−10 °C) was noted at the onset of polymerization. In order to avoid overheating, the reactor was immersed in cold water. After 6 h the polymerization was stopped by fast freezing and opened to air. Solvents were evaporated; the residue was dissolved in chloroform and passed through $Al_2O_3$ column in order to remove copper. After removal of excess of chloroform, the polymer solution was precipitated twice into 10-fold excess of diethyl ether. The formed white powder was collected and dried. The obtained photo-cross-linkable block copolymers (see Figure 2) are further denoted as $PGl_x$-*b*-(PNIPAAm-*r*-$DMIAAm^z)_y$, where *x* and *y* refer to degree of polymerization of the blocks and *z* to the amount (in mol % with respect to the PNIPAAm block) of introduced chromophore (estimated by means of $^1$H NMR spectroscopy). $^1$H NMR ($D_2O$, 500 MHz): $\delta$ (ppm) = 1.0−1.3 (m, $H^g$); 1.3−1.8 (m, $H^d$, $H^h$); 1.8−2.2 (m, $H^e$, $H^i$, $H^o$); 3.45−3.65 (m, $H^a$, $H^b$, $H^c$, $H^j$, $H^k$); 3.7−3.9 (m, $H^f$).

**Synthesis of Nanohydrogels via Photo-Cross-Linking.** Nanohydrogels were obtained by UV irradiation of an aqueous solution of $PGl_x$-*b*-(PNIPAAm-*r*-$DMIAAm^z)_y$ block copolymers using a vertically positioned UV lamp OSRAM (100 W). In order to induce aggregation at elevated temperatures, cross-linking was carried out in a well-thermostated double-wall glass reactor, under stirring.

*General Procedure*. Stock solutions of 5 g/L were prepared by dissolving 0.1 g of $PGl_x$-*b*-(PNIPAAm-*r*-$DMIAAm^z)_y$ block copolymer in 20 mL of water purified by a Millipore system. Solutions of lower concentration were prepared by diluting the stock solution with proper amounts of water. Freshly prepared copolymer solutions were passed through 0.2 $\mu$m nylon membrane filter and transferred to 100 mL double-layer glass reactor. The temperature in of the circulating water in the reactor was already set to 45 or 55 °C. The polymer solutions were thermostated for 30 min at elevated temperatures in order to ensure temperature-induced aggregation and then placed below vertically fitted UV lamp and irradiated for 45 min. Cross-linking of copolymers with shorter PGl block (DP = 55) was carried out at 45 °C, while nanohydrogels from copolymers with longer PGl segment (DP = 100) were obtained at 55 °C. After that time the reactor was removed from the irradiation area and left to cool down to room temperature. The formed nanohydrogels are denoted as H($PGl_x$-*b*-(PNIPAAm-*r*-$DMIAAm^z)_y$).

To evaluate the influence of irradiation time on cross-linking efficacy, cross-linking was carried out for 1 h. During irradiation samples were drawn at appropriate periods in range from 0 to 60 min. To investigate gel formation by the $^1$H NMR technique polymer samples were prepared in $D_2O$. To confirm cross-linking by dimerization of DMIAAm and to check the influence of UV light on the degradation of investigated block copolymers, samples with similar composition but without incorporated chromophore were also exposedto UV light. For all experiments other synthetic procedures remained unchanged.

**Characterization.** The molecular weight and molecular weight distribution of soluble polymers were determined by SEC-MALLS measurements at 45 °C in DMF containing 1 mmol/L LiBr with a nominal flow rate of 1 mL/min. Performing measurements in DMF as mobile phase column system III (GRAM 30 Å, $10^2$ Å, $10^3$ Å (Polymer Standards Service)) with refractive index detector (Δn-1000 RI, WGE Dr. Bures) and a multiangle light scattering detector (DAWN EOS, Wyatt Technologies ($\lambda$ = 690 nm)) was used. Results were evaluated using the ASTRA 4.73 software from Wyatt Technologies. Since estimation of molecular weight according to SEC-MALLS measurements require the knowledge of refractive indices the d*n*/d*c* values of $PGl_x$-*b*-(PNIPAAm-*r*-$DMIAAm^z)_y$ copolymers were calculated according the following equation

$$\frac{dn}{dc} = w_A\left(\frac{dn}{dc}\right)_A + w_B\left(\frac{dn}{dc}\right)_B \quad (1)$$

where $w_A$ and $w_B$ are mass fraction of pure polymers PNIPAAm and poly(glycidol) and $(dn/dc)_A$ and $(dn/dc)_B$ their refractive index increments in DMF, respectively.[33] Values of d*n*/d*c* in DMF were found to be 0.055 mL/g for pure poly(glycidol) and 0.0748 mL/g for PNIPAAm.[32] Since only small amounts of DMIAAm were introduced into copolymer structure, its influence on d*n*/d*c* value of copolymer was neglected.

**$^1$H NMR Spectra Were Recorded on Bruker DRX 500 in $D_2O$.** Calorimetric measurements (DSC) were performed using a 2920 modulated differential scanning calorimeter (TA Instruments). 5.0 g/L polymer aqueous solutions were scanned in sealed DSC cells from 0 to 80 °C in a $N_2$ gas flow against an empty reference cell with heating rates of 5 °C/min.

UV−vis measurements were performed using a Lambda 19 (Perkin-Elmer) spectrometer. Polymer samples with concentration of 2 wt % were investigated at room temperature in the wavelength range from 300 to 500 nm. The values obtained for $\lambda$ = 304 nm were comprised with calibration curve prepared for DMIAAm to give mol % of chromophore in the polymer backbone.

Dynamic light scattering (DLS) studies were performed on a commercially laser light scattering spectrometer (ALV/DLS/SLS-5000) equipped with an ALV-5000EP multiple digital correlator. A laser goniometer system ALV/CGS-8F S/N 025 with a helium−neon laser (Uniphase 1145P, output power of

**Table 2. Characterization of $PGl_x$-*b*-(PNIPAAm-*r*-$DMIAAm^z)_y$ Photo-Cross-Linkable Copolymers by $^1H$ NMR Spectroscopy and SEC-MALLS Measurements**

| | | targeted | | $^1H$ NMR spectroscopy | | | SEC-MALLS | | |
|---|---|---|---|---|---|---|---|---|---|
| sample | $DP_{PGl}$ | $DP_{PNIPAAm}$ | DMIAAm[a] [mol %] | $DP_{PNIPAAm}$ | DMIAAm[a] [mol %] | $M_n$ [g/mol] | d*n*/d*c*[b] | $M_n$ [g/mol] | $M_w/M_n$ |
| $PGl_{55}$-*b*-(PNIPAAm-*r*-$DMIAAm^{5.2})_{110}$ | 55 | 110 | 5.0 | 110 | 5.2 | 17 700 | 0.069 | 40 000 | 1.6 |
| $PGl_{55}$-*b*-(PNIPAAm-*r*-$DMIAAm^{4.7})_{160}$ | 55 | 165 | 5.0 | 160 | 4.7 | 23 900 | 0.071 | 40 000 | 1.5 |
| $PGl_{55}$-*b*-(PNIPAAm-*r*-$DMIAAm^{4.9})_{340}$ | 55 | 330 | 5.0 | 340 | 4.9 | 46 200 | 0.073 | 69 700 | 1.5 |
| $PGl_{55}$-*b*-(PNIPAAm-*r*-$DMIAAm^{9.0})_{170}$ | 55 | 165 | 10.0 | 170 | 9.0 | 26 700 | 0.071 | 45 000 | 1.6 |
| $PGl_{55}$-*b*-(PNIPAAm-*r*-$DMIAAm^{9.0})_{280}$ | 55 | 330 | 10.0 | 280 | 9.0 | 41 300 | 0.072 | 53 000 | 1.5 |
| $PGl_{100}$-*b*-(PNIPAAm-*r*-$DMIAAm^{2.0})_{190}$ | 100 | 200 | 2.0 | 190 | 2.0 | 29 700 | 0.070 | 35 400 | 1.4 |
| $PGl_{100}$-*b*-(PNIPAAm-*r*-$DMIAAm^{5.0})_{210}$ | 100 | 200 | 5.0 | 210 | 5.0 | 33 500 | 0.070 | 36 000 | 1.6 |
| $PGl_{100}$-*b*-(PNIPAAm-*r*-$DMIAAm^{5.5})_{320}$ | 100 | 300 | 5.0 | 320 | 5.5 | 47 500 | 0.071 | 73 000 | 1.4 |
| $PGl_{100}$-*b*-(PNIPAAm-*r*-$DMIAAm^{4.9})_{520}$ | 100 | 600 | 5.0 | 520 | 4.9 | 71 800 | 0.073 | 96 900 | 1.3 |

[a] Molar ratio with respect to PNIPAAm segment. [b] For $PGl_x$-*b*-(PNIPAAm-*r*-$DMIAAm^z)_y$ block copolymers calculated from eq 1.

22 mW, with $\lambda = 632.8$ nm) was used. Hydrodynamic radius measurements were performed at the scattering angle 90° ($R_{h,app}$). The value of hydrodynamic radius and polydispersity index (PDI) of the particles were obtained by cumulant analysis while $R_h$ distributions were obtained with CONTIN. Nanohydrogels samples were diluted 10 times before measurements.

Scanning electron microscopy (SEM) measurements were performed on Zeiss GEMINI DSM 289 equipment. Samples were prepared by dropping of diluted nanohydrogel solutions (5 mg/L) on cleaned microscope glass plate and dried in air at room temperature for 24 h. The dried samples were sputtered with 3 nm thin gold layer prior to observation.

## Results and Discussion

The stabilization of the aggregates deriving from the copolymer structure by itself, followed by freezing of the structure by cross-linking, is a promising direction for formation of nanohydrogels under surfactant-free conditions. Here we describe the synthesis of PGl/PNIPAAm core−shell nanohydrogels with PNIPAAm cross-linked core based on the cross-linking procedure described in the literature.[20,21]

**Synthesis of Photo-Cross-Linkable $PGl_x$-*b*-(PNIPAAm-*r*-$DMIAAm^z)_y$ Block Copolymers.** The first step of nanohydrogels synthesis was the preparation of well-defined photo-cross-linkable $PGl_x$-*b*-(PNIPAAm-*r*-$DMIAAm^z)_y$ block copolymers. Such polymers were obtained using an analogous synthetic route as was described previously for PGl-*b*-PNIPAAm block copolymers.[32] However, for these studies the photo-cross-linkable DMIAAm chromophore was incorporated into the PNIPAAm segment. Two chromophore molecules are needed to form one cross-linking point. Though, in order to form network, at least four chromophore moieties had to be incorporated into one polymer backbone determining the minimum chromophore content of the PNIPAAm block. DMIAAm was used because of a few facts: (i) the reactivity coefficients of DMIAAm with NIPAAm in copolymerization are similar ensuring uniform random composition of copolymers,[34] (ii) DMIAAm is less hydrophobic then most of the photo-cross-linking agents and thus should not significantly affect the value of PNIPAAm transition temperature,[20] and (iii) DMIAAm is temperature and chemical stable with simultaneous ability to follow [2 + 2] cycloaddition under exposure to UV light.[20,21]

A series of photo-cross-linkable block copolymers were prepared changing the PGl macroinitiator length and the molar ratio between the PGl and PNIPAAm blocks. Furthermore, the amount of DMIAAm chromophore incorporated into the PNIPAAm block was also varied. It has to be kept in mind that the minimal mol % amount of chromophore in PNIPAAm block needed to network formation was dependent on the polymer structure (length of PNIPAAm block in copolymers) and had to be set for each block copolymer composition separately. Thus, the DMIAAm content was fixed to 5 and 10 mol % for copolymers $PGl_{55}$-*b*-(PNIPAAm-$DMIAAm^z)_y$ and to 2 and 5 mol % for $PGl_{100}$-*b*-(PNIPAAm-$DMIAAm^z)_y$ copolymers. The detailed characteristics of copolymers are presented in Table 2.

As can be seen from Table 2, the molecular weights calculated from $^1H$ NMR were close to targeted values while values measured by SEC-MALLS chromatography were significantly higher than expected. A similar tendency was already observed for chromophore free analogues (PGl-*b*-PNIPAAm block copolymers) and can be assigned to difficulties in SEC measurements of polymers containing PNIPAAm segments.[32]

The obtained SEC chromatograms were monomodal, confirming successful initiation of the polymerization of the mixture of NIPAAm and DMIAAm by the PGl macroinitiators. The decrease of the elution volume was observed as the molecular weight of the copolymers increased. Additionally, when higher chromophore contents were used in the feed mixture, a decrease in conversion was obtained. This was especially pronounced in case of copolymers containing long PNIPAAm segments. The reason for this might be the DMIAAm double bond which is able to react with the growing polymer radical but due to steric hindrance cannot easily transfer the functionality to the next monomer.[34] The equilibrium between the dormant and active species of polymerizing chain was perturbed. As a result growth of the polymer chain was slowed down, conversion decreased and $M_w/M_n$ values increased.

The amount of chromophore incorporated into PNIPAAm block was calculated independently by $^1H$ NMR spectroscopy and UV−vis measurements. The results are presented in Table 3.

UV−vis absorbance of DMIAAm can be seen in the region 270−310 nm with characteristic maximum at $\lambda = 304$ nm. The absorbance measured for block copolymers was compared with the calibration curve to give the concentration of chromophore in the polymer backbone. Knowing the composition of the copolymers, the mole content of chromophore in the PNIPAAm block was calculated (calculations not included).

In case of $^1H$ NMR measurements estimation of chromophore content was more complex as peaks deriving from chromophore overlapped with peaks deriving from NIPAAm repeating unit (see Figures 3 and 2 for polymer structure).

In the region 1.8−2.2 ppm the signal of two CH protons (e + i) from NIPAAm and DMIAAm repeating unit and of two methyl groups (o) (six protons) from DMIAAm

**Table 3. Chromophore Content and $T_c$ Values of $PGl_x$-*b*-(PNIPAAm-*r*-$DMIAAm^z)_y$ Block Copolymers**

| sample | DMIAAm [mol %] $^1$H NMR | DMIAAm [mol %] UV−vis | $T_c$[a] [°C] DSC |
|---|---|---|---|
| $PGl_{55}$-*b*-(PNIPAAm-*r*-$DMIAAm^{5.2})_{110}$ | 5.2 | 5.2 | 32.5 |
| $PGl_{55}$-*b*-(PNIPAAm-*r*-$DMIAAm^{4.7})_{160}$ | 4.7 | 4.7 | 32.0 |
| $PGl_{55}$-*b*-(PNIPAAm-*r*-$DMIAAm^{4.9})_{340}$ | 4.9 | 5.0 | 31.0 |
| $PGl_{55}$-*b*-(PNIPAAm-*r*-$DMIAAm^{9.0})_{170}$ | 9.0 | 9.2 | 28.0 |
| $PGl_{55}$-*b*-(PNIPAAm-*r*-$DMIAAm^{9.0})_{280}$ | 9.0 | 9.2 | 29.0 |
| $PGl_{100}$-*b*-(PNIPAAm-*r*-$DMIAAm^{2.0})_{280}$ | 2.0 | 2.1 | 33.5 |
| $PGl_{100}$-*b*-(PNIPAAm-*r*-$DMIAAm^{5.0})_{210}$ | 5.0 | 4.9 | 34.0 |
| $PGl_{100}$-*b*-(PNIPAAm-*r*-$DMIAAm^{5.5})_{320}$ | 5.5 | 5.1 | 32.0 |
| $PGl_{100}$-*b*-(PNIPAAm-*r*-$DMIAAm^{4.9})_{520}$ | 4.9 | 5.0 | 31.0 |

[a] Onset value of the endothermic peak of the heating thermograms.

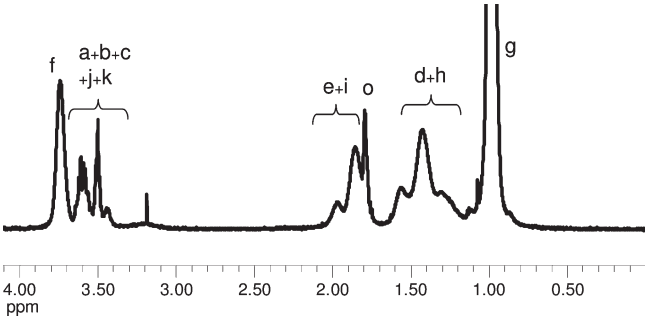


**Figure 3.** $^1$H NMR spectrum of $PGl_{55}$-*b*-(PNIPAAm-*r*-$DMIAAm^{5.2})_{110}$ in $D_2O$.

chromophore could be found. Based on this information, the values of peaks area ($I$) in the region 1.8−2.2 ppm can be calculated as follows:

$$I = I_{\mathrm{NIPAAm}} + 7I_{\mathrm{DMIAAm}} \quad (2)$$

where $I_{\mathrm{NIPAAm}}$ and $I_{\mathrm{DMIAAm}}$ correspond to intensity of PNIPAAm and DMIAAm protons in that region. The value of $I_{\mathrm{NIPAAM}}$ is equal to the value of the signal of the isopropyl proton (f) in the region 3.7−3.9 ppm, while $I_{\mathrm{DMIAAm}}$ can be described as $I_{\mathrm{NIPAAm}}x_{\mathrm{mol(DMIAAm)}}$, where $x_{\mathrm{mol(DMIAAm)}}$ corresponds to the mol % of chromophore in the PNIPAAm block. Hence, $x_{\mathrm{mol(DMIAAm)}}$ was calculated as presented in eq 3.

$$x_{\mathrm{mol(DMIAAm)}} = \frac{I - I_{\mathrm{NIPAAm}}}{7I_{\mathrm{NIPAAm}}} \times 100 \quad (3)$$

Results from both methods were well in accordance (Table 3). Thus, for clarity, the chromophore content in copolymer structure was assigned as obtained from the $^1$H NMR technique.

The influence of chromophore content on the thermal response of block copolymers was investigated by means of DSC (Table 3). The $T_c$ value was estimated as the onset value of the endothermic peak of the heating thermogram. It was observed that with increase of the chromophore content only slight decrease of the phase separation temperature occurred for similar composition of block copolymers. This behavior was in contrast to the behavior observed for photo-cross-linkable PNIPAAm homopolymers, where with increase of chromophore content a much stronger decrease in $T_c$ was reported.[20] This difference was assigned to the copolymer structure. In case of $PGl_x$-*b*-(PNIPAAm-*r*-$DMIAAm^z)_y$ copolymers, two opposite effects seems to influence the $T_c$ value of copolymers. On one hand, the presence of hydrophilic PGl segment shifts $T_c$ of PNIPAAm to higher values; on the other hand, the insertion of hydrophobic chromophore compensates for this effect. As a result, cloud point values of all investigated block copolymers were only slightly affected by incorporation of hydrophobic chromophore and varied from 32 to 37 °C.

**Synthesis of Core−shell Temperature-Sensitive Nanohydrogels.** The PGl/PNIPAAm core−shell nanohydrogels were obtained using the procedure, which can be briefly summarized as follows: at given concentration, a solution of photo-cross-linkable temperature-sensitive $PGl_x$-*b*-(PNIPAAm-*r*-$DMIAAm^z)_y$ copolymer was heated above $T_c$ and was irradiated with UV light to introduce cross-linking points by [2 + 2] cyclodimerization of DMIAAm chromophores (Figure 1). At elevated temperatures the PNIPAAm segments of block copolymer aggregated, and chromophores incorporated in the PNIPAAm segments got close to each other, ensuring short interchain distances between DMIAAm chromophores, while the highly hydrophilic PGl shell provided sufficient stabilization of aggregates for cross-linking. Under such conditions the efficacy of cross-linking was high.

Different techniques were used to investigate the formation of cross-linking points in the PNIPAAm block: (i) $^1$H NMR spectroscopy for observations of internal structure changes, (ii) dynamic light scattering (DLS) for hydrodynamic radii investigation, and (iii) scanning electron microscopy (SEM) to visualize the formation of nanohydrogels. The influence of parameters such as irradiation time, polymer concentration, temperature, copolymer composition, and chromophore content on cross-linking efficacy is discussed below.

**Influence of Temperature on Cross-Linking of DMIAAm Chromophores.** Since the preparation method was based on a microphase separation phenomenon, the influence of temperature on nanohydrogel synthesis was investigated as the first factor. It is well-known from the literature that the heating rate plays an important role in aggregate formation, significantly influencing their size.[34] Since the formation of nanohydrogels with small diameter was desired, solutions of copolymers were heated by one jump from RT to desired temperature (45, 50, or 55 °C) and irradiated with UV light for 1 h.

Two samples, $PGl_{55}$-*b*-(PNIPAAm-*r*-$DMIAAm^{4.7})_{160}$ and $PGl_{100}$-*b*-(PNIPAAm-*r*-$DMIAAm^{5.5})_{320}$, having similar content of chromophore (∼5 mol %) and similar PGl/PNIPAAm block ratio (∼1:3) but different PGl block length (DP = 55 and 100), were chosen for first studies. The formation of nanohydrogels was first investigated at 45 °C, the temperature higher than the phase transition temperature of all investigated block copolymers (see Table 3). Under such conditions nanohydrogels were formed from photo-cross-linkable homo-PNIPAAm polymers.[20,21] The investigations showed at 45 °C the complete chromophore consumption which was confirmed by $^1$H NMR (see also Figure 6). However, formation of monomodal, narrowly distributed nanohydrogels was observed only, when the block copolymer aggregates with shorter poly(glycidol) block ($PGl_{55}$-*b*-(PNIPAAm-*r*-$DMIAAm^{4.7})_{160}$) were cross-linked (Figure 4).

45 °C was not sufficient to form monomodal, well-defined nanohydrogel from block copolymer with longer poly(glycidol) block ($PGl_{100}$-*b*-(PNIPAAm-*r*-$DMIAAm^{5.5})_{320}$) (Figure 5A). If cross-linking was carried out under these conditions, DLS measurements after cross-linking showed a trimodal $R_h$ distribution function. Besides the expected nanohydrogel peak, additional peaks corresponding to non-cross-linked polymer and partially cross-linked polymer

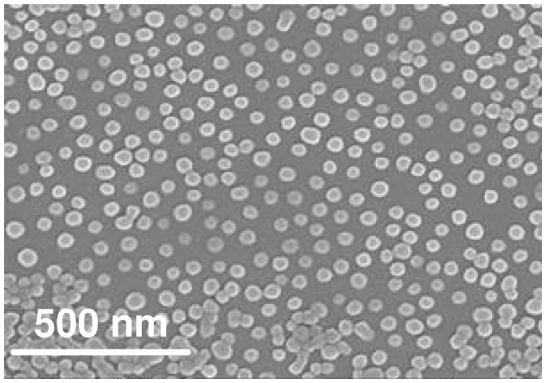


**Figure 4.** SEM image of H($PGl_{55}$-*b*-(PNIPAAm-*r*-$DMIAAm^{4.7}$)$_{160}$) prepared at 45 °C.

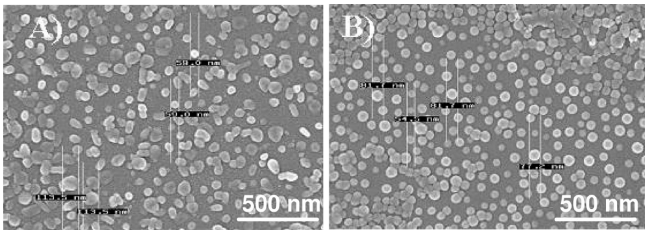


**Figure 5.** SEM images of H($PGl_{100}$-*b*-(PNIPAAm-*r*-$DMIAAm^{5.5}$)$_{320}$) prepared at 45 °C (A) and 55 °C (B).

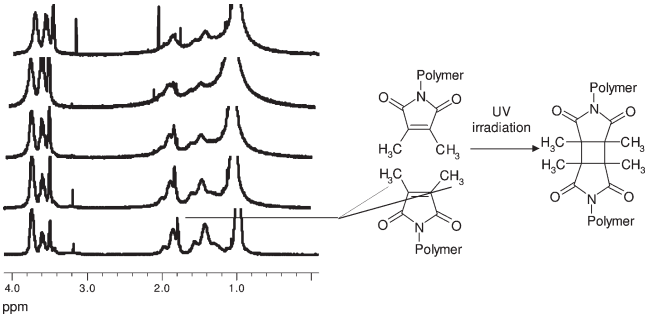


**Figure 6.** Formation of nanohydrogel observed by $^1$H NMR spectroscopy upon cross-linking of $PGl_{55}$-*b*-(PNIPAAm-*r*-$DMIAAm^{4.7}$)$_{160}$.

chains were also observed (data not included). The cloud point temperature depended on the composition of the investigated block copolymers and increased with decreasing relative length of the PNIPAAm block in PGl−PNIPAAm copolymers. These findings can be correlated with the behavior of homo-PNIPAAm with similar molecular weights, indicating that the influence of PGl on the local environment and phase separation of PNIPAAm chains is in the order of a low molecular weight end group. Since block copolymers with a longer PGl chain possess an elevated transition temperature, this observation might be due to incomplete aggregation of the PNIPAAm chains. However, the increase of the cross-linking temperature to 50 °C brought only slight improvement of the system. But when cross-linking of aggregates formed by $PGl_{100}$-*b*-(PNIPAAm-*r*-$DMIAAm^{5.5}$)$_{320}$ was carried out at 55 °C, the formation of monomodal, narrowly distributed nanohydrogels was observed (Figure 5B).

Our investigations clearly show that attached PGl chain strongly affects the local environment and, hence, the phase separation behavior of PNIPAAm segment in $PGl_x$-*b*-(PNIPAAm-*r*-$DMIAAm^z$)$_y$ block copolymers. Generally, above $T_c$ hydrophobic interactions within PNIPAAm chains dominate and the polymer collapse. At those elevated temperatures, water molecules are expelled from the internal space of hydrophobic cores and collapsed PNIPAAm chains get close to each other. In case if chromophores are incorporated into PNIPAAm chain upon aggregation, their molecules are getting closer as well. To form covalent bonds, the chromophore moiety in its excited state must react with another chromophore molecule within the short lifetime. It is possible only if the density of hydrophobic core and the distance between polymer backbones reach the required critical value.

The value of average chain density ($\rho_{particle}$) for collapsed PNIPAAm was found to be 0.35 g/cm$^3$.[35] In contrast to the homopolymer, PNIPAAm grafted with poly(ethylene oxide) formed aggregates with considerably lower chain density,[36] which was attributed to the existence of the low-density hydrophilic PEO shell. In case of $PGl_x$-*b*-(PNIPAAm-*r*-$DMIAAm^z$)$_y$ block copolymers above $T_c$ the aggregation forces in PNIPAAm cores are suppressed by the solubilizing effect of highly hydrophilic PGl chains covalently attached to the collapsed PNIPAAm segment. As a result, the density of the collapsed core decreased and the distance between chromophore moieties become larger leading to a decrease of cross-linking efficacy. This effect was too weak to influence the formation of nanohydrogels from copolymers with shorter PGl block; however, it might be observed in the direct vicinity of $T_c$. In the case of copolymers with longer PGl formation of monomodal nanohydrogels at 45 °C within 1 h was incomplete. The solubilizing effect of poly(glycidol) on the PNIPAAm core could be however suppressed by increasing of the temperature, leading to complete collapse of PNIPAAm chains. As a result, also block copolymers with longer PGl chains could be used for preparation of monomodal nanohydrogels by UV cross-linking within a few minutes.

**Influence of Irradiation Time and Chromophore Content.** The rate of cross-linking was followed independently by three methods: $^1$H NMR, DLS, and SEM. The goal was to optimize the irradiation time in such a manner that the cross-linking of all chromophore molecules in the polymer proceeds without polymer degradation. For investigation two samples with similar composition (PGl/PNIPAAm ratio ∼1:3) but with different chromophore content, $PGl_{55}$-*b*-(PNIPAAm-*r*-$DMIAAm^{4.7}$)$_{160}$ and $PGl_{55}$-*b*-(PNIPAAm-*r*-$DMIAAm^{9.0}$)$_{170}$, were used.

The cross-linking of $PGl_{55}$-*b*-(PNIPAAm-*r*-$DMIAAm^{4.7}$)$_{160}$ by formation of cyclobutane rings of two DMIAAm chromophore moieties was confirmed by $^1$H NMR spectroscopy in deuterated water.[37,38] As cross-linking appeared, the gradual disappearance of the signal of the chromophore methyl group at 1.9 ppm was observed (Figure 6). Additionally, the broadening of all PNIPAAm chain signals was noticed a characteristic feature of network formation. However, due to the signal overlap of the methyl groups with the PNIPAAm backbone, the precise time for complete dimerization of chromophore molecules could not be estimated from the NMR method.

The influence of irradiation time on cross-linking process was further investigated with the DLS technique. The change of hydrodynamic radius distribution of nanohydrogels over time and apparent hydrodynamic radius plotted vs time of irradiation are presented in Figures 7 and 8.

As can be seen, UV-induced cross-linking of DMIAAm chromophore was a fast and efficient process. Just after 1 min formation of nanohydrogel was observed. However, at this stage of the cross-linking two other peaks of non-cross-linked or slightly cross-linked copolymers were also observed. By further increase of irradiation time the additional

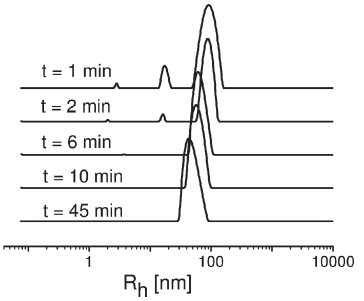


**Figure 7.** Hydrodynamic radius distribution at $\theta = 90°$ at different irradiation times by cross-linking of $PGl_{55}$-*b*-(PNIPAAm-*r*-$DMIAAm^{4.7}$)$_{160}$. Samples were measured at RT.

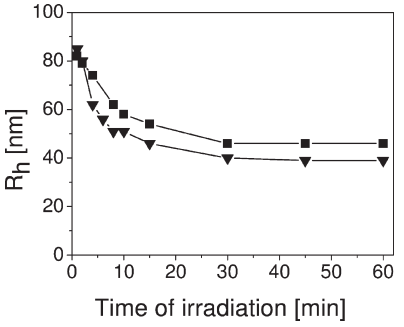


**Figure 8.** Change of the apparent hydrodynamic radius with time for cross-linking of $PGl_{55}$-*b*-(PNIPAAm-*r*-$DMIAAm^{4.7}$)$_{160}$ (■) and $PGl_{55}$-*b*-(PNIPAAm-*r*-$DMIAAm^{9.0}$)$_{170}$ (▼). Lines were added to guide the eyes.

two peaks disappeared gradually, and after 6 min only one peak deriving from nanohydrogel particle remained. Nevertheless, after 6 min the cross-linking was not completed. By further irradiation the nanohydrogel size was still changing gradually shifting to lower values (Figure 8). The gradual decrease of hydrodynamic radius of the particles could be understood as further cross-linking process and formation of a more compact microstructure of nanohydrogel. Finally, after 30 min the diameter of the nanohydrogel remained unchanged, confirming full intrachain dimerization of incorporated chromophores.

It is worth mentioning that the rate of cross-linking appeared to be independent of chromophore content. The hydrodynamic radius of samples with 5 and 9 mol % of chromophore reached a constant size within nearly the same time of irradiation (Figure 8). As expected, the chromophore content influenced the final size of the nanohydrogels. For the corresponding PGl/PNIPAAm ratio of block copolymers, the nanohydrogels with higher degree of cross-linking, obtained from block copolymer containing 9 mol % of chromophore, exhibited smaller dimensions. It is noteworthy that in each case monodispersed, well-defined nanohydrogel particles with narrow size distribution were observed.

The progress of cross-linking was also followed by SEM (Figure 9). The results corresponded well to those obtained by DLS measurements. After 2 min (Figure 9A) nonspherical submicrometer-sized structures of nanohydrogels and partially cross-linked polymer were formed. After 4 min of UV-irradiation (Figure 9B) still not uniform particles were detected, while after 6 min for the first time particles with spherical morphology were observed (Figure 9C). Upon further irradiation a similar tendency like during DLS measurements was observed; i.e., the increase of irradiation time resulted in a decrease of the size of nanohydrogels (in

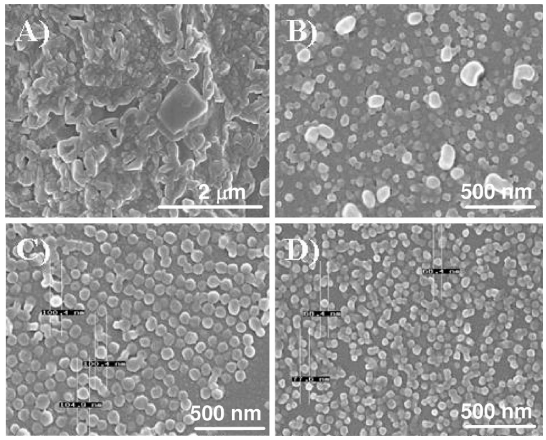


**Figure 9.** SEM images of nanohydrogel formation from $PGl_{55}$-*b*-(PNIPAAm-*r*-$DMIAAm^{4.7}$)$_{160}$ after 2 (A), 4 (B), 6 (C), and 45 min (D).

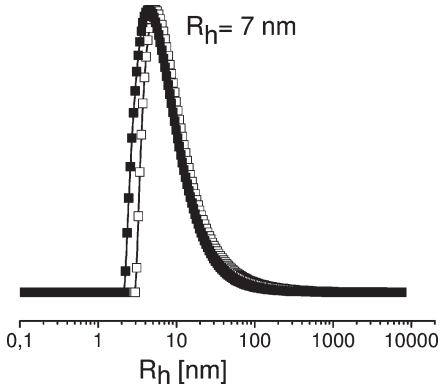


**Figure 10.** Hydrodynamic radius distribution at $\theta = 90°$ at RT of $PGl_{55}$-*b*-$(PNIPAAm)_{170}$ before (□) and after (■) UV irradiation for 1 h.

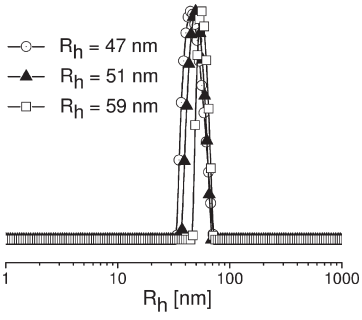


**Figure 11.** Hydrodynamic radius distribution ($\theta = 90°$) of H($PGl_{55}$-*b*-(PNIPAAm-*r*-$DMIAAm^{4.7}$)$_{160}$) nanohydrogels at RT synthesized at concentrations of 0.1 (○), 5 (▲), and 10 g/L (□).

dry state) from 100 nm (Figure 9C) to 70 nm (Figure 9D) with simultaneous reform of particle morphology.

The irradiation time needed for full consumption of chromophore was longer than for PNIPAAm copolymers having no block structure.[20] Such differences may be assigned to the structure of aggregates formed above $T_c$. As already discussed for $PGl_x$-*b*-(PNIPAAm-*r*-$DMIAAm^z$)$_y$ copolymers, the density of the collapsed PNIPAAm core is lower than for homo-PNIPAAm. Less compact cores results in lower probability of efficient chromophore dimerization and therefore decreasing the cross-linking rate.

**Influence of UV Light on Block Copolymer Properties.** An important question was also if cross-linking points in nanohydrogels were formed only as the result of dimerization of

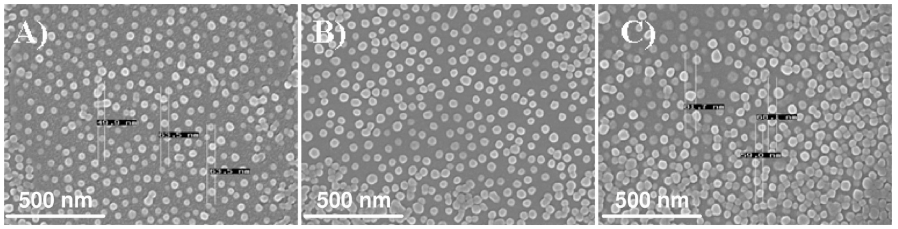


**Figure 12.** SEM pictures of $H(PGl_{55}$-*b*-(PNIPAAm-*r*-$DMIAAm^{4.7})_{160})$ nanohydrogels obtained at concentrations of 0.1 (A), 5 (B), and 10 g/L (C).

DMIAAm chromophore molecules incorporated into $PGl_x$-*b*-(PNIPAAm-*r*-$DMIAAm^z)_y$ copolymers or by formation of undefined covalent bonds between copolymer chains upon exposure to UV light. Hence, the analogous block copolymer $PGl_{55}$-*b*-$PNIPAAm_{170}$ without incorporated chromophores was exposed to UV light at the same experimental conditions as used upon cross-linking process. The hydrodynamic radius distribution of $PGl_{55}$-*b*-$PNIPAAm_{170}$ solution before and after UV irradiation is presented in Figure 10.

The DLS measurements clearly showed that both the size of measured block copolymers and the hydrodynamic radius distribution of copolymer were not influenced by UV irradiation. Additionally, after exposure to UV light no additional peaks indicating cross-linking were found, excluding possible undesired cross-linking between copolymer chains. These results confirmed two important facts: (i) formation of nanohydrogels from $PGl_x$-*b*-(PNIPAAm-*r*-$DMIAAm^z)_y$ copolymers occurred only by chromophore dimerization and (ii) stability of copolymers to applied dose of UV light.

**Influence of Block Copolymer Concentration.** The last investigated parameter, which could influence the nanohydrogel formation, was the concentration of polymer in solution used for photo-cross-linking. Generally, the size of aggregates formed from stimuli-sensitive polymers increases significantly as the concentration of polymer in the solution increases. At higher polymer concentrations, under the same cross-linking conditions, i.e., heating rate or temperature, individual chains have more chances to aggregate and may form larger and suspended particles. On the other hand, at higher concentrations intermicellar cross-linking leading to uncontrolled increase of particle size may occur. Thus, usually synthesis of nanohydrogels is carried out in diluted system, often much lower than 5 g/L.[22]

In Figure 11 the hydrodynamic radius distributions and in Figure 12 SEM pictures of nanohydrogels obtained from $PGl_{55}$-*b*-(PNIPAAm-*r*-$DMIAAm^{4.7})_{160}$ copolymer at three different concentrations (0.1, 5, and 10 g/L) are presented. As can be seen, spherical, monomodal, narrowly distributed nanohydrogels were obtained at all investigated polymer concentration. The size of nanohydrogels increased as polymer concentration increased, however only slightly. A 100 times increase of concentration resulted in change of nanohydrogel diameter from 47 to 59 nm. Cross-linking at high polymer concentration in solution was only possible because of unique properties of developed system. The efficient stabilization of aggregates at elevated temperatures by the surrounding, highly hydrophilic poly(glycidol) shell allowed us not only to cross-link the block copolymers under applied conditions but also to prevent interaggregate cross-linking of hydrophobic PNIPAAm core at elevated temperatures and high copolymer content in solution.

**Summary.** Evaluating the obtained results, the optimal cross-linking conditions for formation of nanohydrogels from $PGl_x$-*b*-(PNIPAAm-*r*-$DMIAAm^z)_y$ block copolymers were (i) temperature 45 °C for copolymers with shorter PGl block (DP = 55) or 55 °C for copolymers with longer PGl block (DP = 100), (ii) polymer concentration of 5 g/L, and (iii) 45 min UV irradiation time. Under these conditions well-defined, stable, narrowly distributed particles with the hydrodynamic radius values in nanorange scale were obtained. The hydrodynamic radius of nanohydrogels is presented in Table 4. As can be seen in Table 4, the size of nanohydrogels was influenced by copolymer composition, length of blocks, and degree of cross-linking. As expected, hydrodynamic radius of nanohydrogels increased with increasing PGl/PNIPAAm ratio, e.g., increasing length of PNIPAAm block in copolymer. Furthermore, samples with higher degree of cross-linking showed smaller sizes (for similar copolymer composition).

**Table 4. Apparent Hydrodynamic Radius of Nanohydrogels Obtained by UV Irradiation of Photo-Cross-Linkable $PGl_x$-*b*-(PNIPAAm-*r*-$DMIAAm^z)_y$ Block Copolymers ($R_h$ Measured at RT)**

| sample | $R_{h,app}$ [nm] |
|---|---|
| $H(PGl_{55}$-*b*-(PNIPAAm-*r*-$DMIAAm^{5.2})_{110})$ | 36 |
| $H(PGl_{55}$-*b*-(PNIPAAm-*r*-$DMIAAm^{4.7})_{160})$ | 52 |
| $H(PGl_{55}$-*b*-(PNIPAAm-*r*-$DMIAAm^{4.9})_{340})$ | 64 |
| $H(PGl_{55}$-*b*-(PNIPAAm-*r*-$DMIAAm^{9.0})_{170})$ | 38 |
| $H(PGl_{55}$-*b*-(PNIPAAm-*r*-$DMIAAm^{9.0})_{280})$ | 47 |
| $H(PGl_{100}$-*b*-(PNIPAAm-*r*-$DMIAAm^{2.0})_{280})$ | 93 |
| $H(PGl_{100}$-*b*-(PNIPAAm-*r*-$DMIAAm^{5.0})_{210})$ | 61 |
| $H(PGl_{100}$-*b*-(PNIPAAm-*r*-$DMIAAm^{5.5})_{320})$ | 64 |
| $H(PGl_{100}$-*b*-(PNIPAAm-*r*-$DMIAAm^{4.9})_{520})$ | 66 |

## Conclusions

In our studies a new method of nanohydrogel synthesis from temperature-sensitive block copolymers under surfactant-free conditions and high solid content was developed. Novel core−shell nanohydrogels with cross-linked PNIPAAm core and hydrophilic PGl shell were obtained by UV irradiation of photo-cross-linkable block copolymers above their phase separation temperatures ($T_c$) in aqueous solution. The presence of the highly hydrophilic PGl shell prevented precipitation of collapsed PNIPAAm cores at elevated temperatures, efficiently stabilizing temperature-induced aggregates and enabling intramicellar cross-linking.

The first step of nanohydrogels preparation included the synthesis of photo cross-linkable block copolymers with different PGl block length, amount of chromophore (DMIAAm), and PGl/PNIPAAm block ratio. By combination of anionic and controlled radical polymerization, well-defined block copolymers as network precursors with targeted composition were obtained. The incorporation of chromophores into the PNIPAAm block only slightly influenced the $T_c$ value of block copolymers.

$^1$H NMR, DLS, and SEM techniques were used to follow and confirm UV-induced cross-linking of aggregates and the formation of nanohydrogels. The efficacy and rate of cross-linking were almost independent of chromophore content and copolymer composition but strongly dependent on length of PGl chains in the sample. The cross-linking carried out at 45 °C led to monomodal well-defined core−shell nanohydrogels for block

copolymers with shorter PGl segment (DP = 55). Cross-linking of copolymers with longer PGl blocks (DP = 100) under identical conditions was not efficient and led to broadly distributed products. This was caused by the fact that the presence of hydrophilic PGl significantly decreased the density of the PNIPAAm core and, thus, the distance between chromophore moieties decreasing rate and efficiency of cross-linking. However, this could be overcome by increase of the cross-linking temperature to 55 °C, enabling the formation of well-defined, monomodal nanohydrogels also from block copolymers with longer PGl segments. For the copolymers with similar composition the size of nanohydrogels decreased with increasing degree of cross-linking. Furthermore, the size of nanohydrogels increased with increasing PGl/PNIPAAm ratio, e.g., increasing length of PNIPAAm blocks in copolymers used for cross-linking. Of great importance was the fact that all nanohydrogels were stable after synthesis and did not precipitate from the solution even after long storage times.

**Acknowledgment.** The authors appreciate the support of the Polish Ministry of Scientific Research and Information Technology (Grant 4T09A05225) and the European Graduate College "Advanced Polymer Materials" (EGC 720) founded by Deutsche Forschungsgemeinschaft (DFG). The authors are also thankful to Prof. Dr. K.-F. Arndt (Institute for Physical Chemistry and Electrochemistry, TU Dresden) for the use of DLS and SLS system and Dr. V. Boyko for help in measurements.

## References and Notes

(1) Ballauff, M.; Lu, Y. *Polymer* **2007**, *48*, 1815–1823.
(2) Dupin, D.; Fujii, S.; Armes, S. P.; Reeve, P.; Baxter, S. M. *Langmuir* **2006**, *22*, 3381–3387.
(3) Nayak, S.; Lyon, L. A. *Angew. Chem., Int. Ed.* **2005**, *44*, 7686–7708.
(4) Pelton, R. *Adv. Colloid Interface Sci.* **2000**, *85*, 1–33.
(5) Das, M.; Mardyani, S.; Chan, W. C.; Kumacheva, E. *Adv. Mater.* **2006**, *18*, 80–83.
(6) Lu, Y.; Mei, Y.; Drechsler, M.; Ballauff, M. *Angew. Chem., Int. Ed.* **2006**, *45*, 813–816.
(7) Sahiner, N.; Godbey, W. T.; Mcpherson, G. L.; John, V. T. *Colloid Polym. Sci.* **2006**, *284*, 1121–1129.
(8) Soppimath, K. S.; Tan, D. C.; Yang, Y. *Adv. Mater.* **2005**, *17*, 318–323.
(9) Shibayama, M.; Tanaka, T. *Adv. Polym. Sci.* **1993**, *109*, 1–62.
(10) Snowden, M.; Marston, N.; Vincent, B. *Colloid Polym. Sci.* **1994**, *272*, 1273–1280.
(11) Saunders, B.; Vincent, B. *J. Chem. Soc., Faraday Trans.* **1996**, *92*, 3385–3389.
(12) Pankasem, S.; Thomas, J. K.; Snowden, M. J.; Vincent, B. *Langmuir* **1994**, *10*, 3023–3026.
(13) Gan, D.; Lyon, L. *Macromolecules* **2002**, *35*, 9634–9639.
(14) Duracher, D.; Sauzedde, F.; Elaissari, A.; Perrin, A.; Pichot, C. *Colloid Polym. Sci.* **1998**, *276*, 219–231.
(15) Dingenouts, N.; Norhausen, C.; Ballauff, M. *Macromolecules* **1998**, *31*, 8912–8917.
(16) Shibayama, M. *Macromol. Chem. Phys.* **1998**, *199*, 1–30.
(17) McPhee, W.; Tam, C.; Pelton, R. *J. Colloid Interface Sci.* **1993**, *156*, 24–30.
(18) Tam, K.; Wu, X.; Pelton, R. *J. Polym. Sci., Part A: Polym. Chem.* **1993**, *31*, 963–969.
(19) Elaissaf, J. *J. Appl. Polym. Sci.* **1978**, *22*, 873–874.
(20) Vo, C.; Kuckling, D.; Adler, H.-J.; Schönhoff, M. *Colloid Polym. Sci.* **2002**, *280*, 400–409.
(21) Kuckling, D.; Vo, C.; Wohlrab, S. *Langmuir* **2002**, *18*, 4263–4269.
(22) Kuckling, D.; Vo, C.; Adler, H.-J.; Völkel, A.; Cölfen, H. *Macromolecules* **2006**, *39*, 1585–1591.
(23) Gao, J.; Firsken, B. *Langmuir* **2003**, *19*, 5212–5216.
(24) Wang, B.; Mukataka, S.; Kodama, M.; Kokofuta, E. *Langmuir* **1997**, *13*, 6108–6114.
(25) Hu, T.; Wu, C. *Macromolecules* **2001**, *34*, 6802–6805.
(26) Virtanen, J.; Baron, C.; Tenhu, H. *Macromolecules* **2000**, *33*, 336–341.
(27) Wooley, K. L. *J. Polym. Sci., Part A: Polym. Chem.* **2000**, *38*, 1397–1407.
(28) Guo, A.; Liu, G.; Tao, J. *Macromolecules* **1996**, *29*, 2487–2493.
(29) Kim, J. S.; Youk, J. H. *Polymer* **2009**, *50*, 2204–2208.
(30) Jiang, J.; Qi, B.; Lepage, M.; Zhao, Y. *Macromolecules* **2007**, *40*, 790–792.
(31) Davis, K.; Matyjaszewski, K. *Macromolecules* **2000**, *33*, 4039–4047.
(32) Mendrek, S.; Mendrek, A.; Adler, H.-J.; Dworak, A.; Walach, W.; Kuckling, D. *J. Polym. Sci., Part A: Polym. Chem.* **2008**, *46*, 2488–2499.
(33) Cooper, A. R. *Determination of Molecular Weight*; John Wiley & Sons Ltd.: New York, 1996; p 56.
(34) Kuckling, D.; Adler, H.-J.; Ling, L.; Habicher, W.; Arndt, K. *Polym. Bull.* **2000**, *44*, 269–276.
(35) Kawaguchi, S.; Winnik, M.; Ito, K. *Macromolecules* **1995**, *28*, 1159–1166.
(36) Qiu, X.; Wu, C. *Macromolecules* **1997**, *30*, 7921–7926.
(37) Seifert, S.; Oppermann, W.; Saalwächter, K. *Polymer* **2007**, *48*, 5599–5611.
(38) Xiuling, Y.; Corten, C.; Görner, H.; Wolff, T.; Kuckling, D. *J. Photochem. Photobiol.* **2008**, *198*, 34–44.